Advances in Applied Mathematics and Mechanics
Adv. Appl. Math. Mech., Vol. **10**, No. 1, pp. 41-61

DOI: 10.4208/aamm.OA-2016-0184
February 2018

Numerical Comparison of the LOOCV-MFS and the MS-CTM for 2D Equations

Fang Hao, Hui Lv and Xiaoyan Liu*

College of Mathematics, Taiyuan University of Technology, Taiyuan, Shanxi 030024, China

Received 15 November 2016; Accepted (in revised version) 5 April 2017

Abstract. The method of fundamental solutions (MFS) and the Collocation Trefftz method have been known as two highly effective boundary-type methods for solving homogeneous equations. Despite many attractive features of these two methods, they also experience different aspects of difficulty. Recent advances in the selection of source location of the MFS and the techniques in reducing the condition number of the Trefftz method have made significant improvement in the performance of these two methods which have been proven to be theoretically equivalent. In this paper we will compare the numerical performance of these two methods under various smoothness of the boundary and boundary conditions.

AMS subject classifications: 65M10, 78A48

Key words: Trefftz method, the method of fundamental solution, LOOCV, multiple scale method, non-harmonic boundary conditions.

1 Introduction

The method of fundamental solutions (MFS) [3, 9] and the Collocation Trefftz method (CTM) [14, 26, 27] are considered to be two of the most powerful boundary meshless methods for solving homogeneous equations under the condition that either the fundamental solution or the T-complete functions are available for the given differential equation. One of the great advantages of using these types of boundary-only solution procedure is simplicity. Furthermore, the solution of both of these methods converges exponentially. On the negative side, the MFS has the uncertainty of placing the source points outside the domain. Some improvements proposed like adaptive approach [6, 21] were computational expensive and nonlinear that hard to be solved, they were replaced by later fixed approach [3, 6, 8] to bear mentioned problems. Selection of optimal source

*Corresponding author.
Email: lucyyanxiao@163.com (X. Y. Liu)

location, accuracy of MFS primarily depending on, were dealt with by various algorithms [1,7,24,25]. In particular, the LOOCV (Leave-One-Out Cross Validation) algorithm [23] has been successfully adopted to locate the optimal source points [1]. Collocation Trefftz method is notorious for ill-conditioning of the resultant matrix. In recent years, significant advances have been developed to alleviate these deficiencies. The collocation Trefftz method was proposed to deal with the singularity by adopting nonsingular T-complete basis function [10, 12]. Recently,the so-called multiple scale technique [13–15, 17], a preconditioning technique, has been proposed to reduce the condition number of the resultant matrix for the nonlinear problems. In summary, both the MFS and the Trefftz method have been further enhanced and become more powerful. It is of interest to note that there is a strong mathematical connection between the MFS and the Trefftz method. Chen et al. [2] showed that the MFS and the Trefftz method are theoretically equivalent for solving the Laplace and biharmonic equations for the case of the circular domain. Liu [16] extended the equivalence between the Trefftz method and the MFS to the arbitrary domain. On the other hand, the numerical procedure of these two methods are completely different. Fu [5] has extended the MFS and collocation Trefftz method for solving nonlinear and anisotropic equations, Fu [4] has solved Laplace transformed time fractional diffusion equations which extends MFS and Trefftz Method. To the best of our knowledge, no research has been conducted to compare the performance of LOOCV-MFS and multiple scale CTM numerically. In particular, due to the recent development of the MFS in the selection of the source points and the Trefftz method in the reduction of the condition number, it is the purpose of this paper to study the performance and make a comparison of these two powerful numerical methods. The paper is organized as follows. In Section 2 we describe Laplace equations and biharmonic equations and introduce the modified Trefftz method which has multiple-scale in Trefftz bases to solve the Laplace equation with Dirichlet boundary condition and Biharmonic equation with the first and second kind, respectively. In Section 3 we briefly review the MFS for solving two kinds of equations as shown in Section 2. Numerical comparisons of these two methods have been provided in Section 4. In Section 5 we draw conclusions on the performance and comparison of these two methods.

2 The multiple-scale Trefftz method

2.1 Laplace equation

We consider the following Laplace equation with Dirichlet boundary condition

$$\Delta u(r,\theta) = 0, \qquad (r,\theta) \in \Omega, \tag{2.1a}$$

$$u(x,y) = f(r,\theta), \qquad (r,\theta) \in \partial,\ \Omega, \tag{2.1b}$$

where f is a given function. In the Trefftz method, the solution in Eq. (2.1) can be approximated by the T-complete functions satisfying the governing equation Eq. (2.1a). For the

Laplace equation in the two-dimensional bounded domain, the T-complete functions are as follows:

$$\{1, r^k\cos k\theta, r^k\sin k\theta\}, \quad k=1,2,\cdots,$$

where r and θ are the polar coordinates of the two-dimensional plane. The approximated solution of u in Eq. (2.1) can be represented by a linear combination of the T-complete functions:

$$u(r,\theta)=a_0+\sum_{k=1}^{m}(a_k r^k\cos k\theta+b_k r^k\sin k\theta). \tag{2.2}$$

Let $\{(r_j,\theta_j)\}_{j=1}^{n}$ be the collocation points on $\partial\Omega$. By the collocation method, we have the following system of equations

$$\begin{bmatrix} 1 & r_1\cos\theta_1 & r_1\sin\theta_1 & \cdots & r_1^m\cos m\theta_1 & r_1^m\sin m\theta_1 \\ 1 & r_2\cos\theta_2 & r_2\sin\theta_2 & \cdots & r_2^m\cos m\theta_2 & r_2^m\sin m\theta_2 \\ \vdots & \vdots & \vdots & \ddots & \vdots & \vdots \\ 1 & r_n\cos\theta_n & r_n\sin\theta_n & \cdots & r_n^m\cos m\theta_n & r_n^m\sin m\theta_n \end{bmatrix} \begin{bmatrix} a_0 \\ a_1 \\ b_1 \\ \vdots \\ a_m \\ b_m \end{bmatrix} = \begin{bmatrix} f_1 \\ f_2 \\ f_3 \\ \vdots \\ f_n \end{bmatrix}.$$

The above system of equations can be written in the matrix form

$$\boldsymbol{K}\boldsymbol{a}=\boldsymbol{f}, \tag{2.3}$$

where $\boldsymbol{K}$ is a $n\times(2m+1)$ coefficient matrix, $2m+1$ is the number of T-complete functions, $\boldsymbol{a}=[a_0,a_1,b_1,\cdots,a_m,b_m]^T$ is a $(2m+1)\times 1$ coefficient vector to be determined, and $\boldsymbol{f}$ is an $n\times 1$ matrix. When m becomes large, $\boldsymbol{K}$ in (2.3) is highly ill-conditioned.

Liu [14] first proposed the idea of characteristic length, which can be used to reduce the ill-conditioning of the Trefftz method. Then Liu [18] proposed how to locate the best source points in MFS to equilibrate the matrix. The equilibrated matrix has the minimal condition number resulting from the fact that all the column norms or row norms are the same [20]. If we find fixable multiple-scale $R_0,R_1,\cdots,R_{2m}$ on Eq. (2.3), we could reduce the condition number of $\boldsymbol{K}$. The characteristic length is defined as follows

$$R_{j-1}=\sqrt{\sum_{i=1}^{n}K_{i,j}^2}, \quad j=1,2,\cdots,2m+1,$$

and let

$$u(r,\theta)=\frac{\widehat{a}_0}{R_0}+\sum_{k=1}^{m}\frac{\widehat{a}_k r^k\cos k\theta}{R_{2k-1}}+\sum_{k=1}^{m}\frac{\widehat{b}_k r^k\sin k\theta}{R_{2k}}, \tag{2.4}$$

where $\widehat{a}_0=a_0R_0$, $\widehat{a}_k=a_kR_k$, $\widehat{b}_k=b_kR_{m+k}$. Then $\widehat{\boldsymbol{K}}$ can be represented as follows:

$$\widehat{\boldsymbol{K}}=\begin{bmatrix} \frac{1}{R_0} & \frac{r_1\cos\theta_1}{R_1} & \frac{r_1\sin\theta_1}{R_2} & \cdots & \frac{r_1^m\cos m\theta_1}{R_{2m-1}} & \frac{r_1^m\sin m\theta_1}{R_{2m}} \\ \frac{1}{R_0} & \frac{r_2\cos\theta_2}{R_1} & \frac{r_2\sin\theta_2}{R_2} & \cdots & \frac{r_2^m\cos m\theta_2}{R_{2m-1}} & \frac{r_2^m\sin m\theta_2}{R_{2m}} \\ \vdots & \vdots & \vdots & \ddots & \vdots & \vdots \\ \frac{1}{R_0} & \frac{r_n\cos\theta_n}{R_1} & \frac{r_n\sin\theta_n}{R_2} & \cdots & \frac{r_n^m\cos m\theta_n}{R_{2m-1}} & \frac{r_n^m\sin m\theta_n}{R_{2m}} \end{bmatrix}.$$

Hence, a new matrix system equivalent to Eq. (2.3) is:

$$\widehat{\boldsymbol{K}}\widehat{\boldsymbol{a}}=\boldsymbol{f}, \tag{2.5}$$

where $\widehat{\boldsymbol{a}}=[\widehat{a}_0,\widehat{a}_1,\widehat{b}_1,\cdots,\widehat{a}_m,\widehat{b}_m]^T$.

In order to reduce the condition number of $\widehat{\boldsymbol{K}}$, we adjust this matrix to equilibrate by choosing a suitable R_k. Since the condition number is almost minimum when each column of matrix $\widehat{\boldsymbol{K}}$ is equivalent and the square norm of the each column of matrix $\widehat{\boldsymbol{K}}$ are the same:

$$\sum_{i=1}^{n}\widehat{K}_{i1}^2=\cdots=\sum_{i=1}^{n}\widehat{K}_{in}^2,$$

we could derive R_k from

$$R_k=\gamma\left(\frac{\sum_{i=1}^{n}\widehat{K}_{ik}^2}{\sum_{i=1}^{n}\widehat{K}_{i1}^2}\right)^{1/2}, \tag{2.6}$$

where γ is an amplification factor, ranging from 0.5 to 2, which is applied to reduce the condition number better. For simplicity, let γ be 1. Consequently, Eq. (2.5) can be solved as follows

$$\boldsymbol{A}\boldsymbol{a}=\boldsymbol{f_1},$$

where $\boldsymbol{A}=\widehat{\boldsymbol{K}}^T\widehat{\boldsymbol{K}}$, $\boldsymbol{f_1}=\widehat{\boldsymbol{K}}^T\boldsymbol{f}$.

The above pre-conditioning process will significantly reduce the conditioning number of the matrix system resulting from the Trefftz collocation method. As shown in the section of numerical results, the Trefftz method becomes very stable using the above multiple scale technique.

2.2 Biharmonic equation

In this section, we give a brief review of the multiple-scale Trefftz method. The biharmonic equation of a two-dimensional boundary value problem is as follows:

$$\Delta^2 u(r,\theta)=0, \qquad (r,\theta)\in\Omega, \tag{2.7a}$$

$$u(r,\theta)=f(\theta), \quad \frac{\partial u}{\partial n}(r,\theta)=g(r,\theta), \qquad 0\le\theta\le 2\pi, \tag{2.7b}$$

$$\text{or } u(r,\theta)=f(\theta), \quad \Delta u(r,\theta)=g(r,\theta), \qquad 0\le\theta\le 2\pi, \tag{2.7c}$$

where f and g are given functions. $r(\theta)$ is a function which describes the boundary of the problem domain. Eqs. (2.7a)-(2.7b) is the first biharmonic problem while (2.7a), (2.7c) is the second biharmonic problem.

The T-complete functions for the biharmonic equation in the polar coordinate system are as follows:

$$\{1,r^k\cos k\theta,r^k\sin k\theta,r^2,r^{k+2}\cos k\theta,r^{k+2}\sin k\theta\},\quad k=1,2,\cdots.$$

The multiple-scale characteristic length is added to the above T-complete functions, the approximation of u can be written as

$$\begin{aligned}u(r,\theta)=a_0+\sum_{k=1}^{m}\Big(\frac{a_kr^k\cos k\theta}{R_k}+\frac{b_kr^k\sin k\theta}{R_{k+m}}\Big)\\+\frac{c_0r^2}{R_{2m+1}}+\sum_{k=1}^{m}\Big(\frac{c_kr^{k+2}\cos k\theta}{R_{2m+k+1}}+\frac{d_kr^{k+2}\sin k\theta}{R_{3m+k+1}}\Big).\end{aligned}\tag{2.8}$$

Note that

$$\frac{\partial u(r,\theta)}{\partial n}=\eta(\theta)\left[\frac{\partial u(r,\theta)}{\partial r}-\frac{r'\partial u(r,\theta)}{r^2\partial\theta}\right],$$

where

$$r'=\frac{\partial r}{\partial\theta},\quad \eta(\theta)=\frac{r(\theta)}{\sqrt{r^2(\theta)+(r'(\theta))^2}}.$$

For the first biharmonic problem, we collocate the boundary condition with n boundary points $\{(r_i,\theta_i)\}_{i=1}^n$ and obtain

$$u(r_i,\theta_i)=f(r_i,\theta_i),\quad \frac{\partial u}{\partial n}(r_i,\theta_i)=g(r_i,\theta_i),\quad i=1,\cdots,N.\tag{2.9}$$

Then from Eq. (2.8), we have

$$\frac{\partial u(r_i,\theta_i)}{\partial n}=\frac{2c_0\eta_ir_i}{R_1}+\sum_{k=1}^{m}\left[\frac{a_kE_{ik}}{R_k}+\frac{b_kF_{ik}}{R_{m+k}}+\frac{c_kG_{ik}}{R_{2m+k+1}}+\frac{d_kH_{ik}}{R_{3m+k+1}}\right],\tag{2.10}$$

where

$$\begin{aligned}&E_{ik}=\eta_ir_i^k\left(\frac{k}{r_i}\cos k\theta_i+\frac{kr_i'}{r_i^2}\sin k\theta_i\right),&&F_{ik}=\eta_ir_i^k\left(-\frac{kr_i'}{r_i^2}\cos k\theta_i+\frac{k}{r_i}\sin k\theta_i\right),\\&G_{ik}=\eta_ir_i^{k+2}\left(\frac{k+2}{r_i}\cos k\theta_i+\frac{kr_i'}{r_i^2}\sin k\theta_i\right),&&H_{ik}=\eta_ir_i^{k+2}\left(-\frac{kr_i'}{r_i^2}\cos k\theta_i+\frac{k+2}{r_i}\sin k\theta_i\right).\end{aligned}$$

Put Eq. (2.10) into Eq. (2.8) and Eq. (2.9), we derive a $2n*(4m+2)$ dimensions linear equation system as:

$$\begin{bmatrix}\boldsymbol{A}&\boldsymbol{B}\\\boldsymbol{C}&\boldsymbol{D}\end{bmatrix}\begin{bmatrix}\boldsymbol{a}\\\boldsymbol{b}\end{bmatrix}=\begin{bmatrix}\boldsymbol{f}\\\boldsymbol{g}\end{bmatrix},\tag{2.11}$$

where

$$\boldsymbol{a}=[a_0,a_1,\cdots a_m,b_1,\cdots,b_m]^T,$$
$$\boldsymbol{b}=[c_0,c_1,\cdots,c_m,d_1,\cdots,d_m]^T,$$

are unknown coefficients to be determined, and

$$\boldsymbol{A}=\begin{bmatrix} 1 & \frac{r_1\cos\theta_1}{R_1} & \cdots & \frac{r_1^m\cos m\theta_1}{R_m} & \frac{r_1\sin\theta_1}{R_{m+1}} & \cdots & \frac{r_1^m\sin m\theta_1}{R_{2m}} \\ 1 & \frac{r_2\cos\theta_2}{R_1} & \cdots & \frac{r_2^m\cos m\theta_2}{R_m} & \frac{r_2\sin\theta_2}{R_{m+1}} & \cdots & \frac{r_2^m\sin m\theta_2}{R_{2m}} \\ \vdots & \vdots & \ddots & \vdots & \vdots & \ddots & \vdots \\ 1 & \frac{r_n\cos\theta_n}{R_1} & \cdots & \frac{r_n^m\cos m\theta_n}{R_m} & \frac{r_n\sin\theta_n}{R_{m+1}} & \cdots & \frac{r_n^m\sin m\theta_n}{R_{2m}} \end{bmatrix},$$

$$\boldsymbol{B}=\begin{bmatrix} \frac{r_1^2}{R_{2m+1}} & \frac{r_1^3\cos\theta_1}{R_{2m+2}} & \cdots & \frac{r_1^{m+2}\cos m\theta_1}{R_{3m+1}} & \frac{r_1^3\sin\theta_1}{R_{3m+2}} & \cdots & \frac{r_1^{m+2}\sin m\theta_1}{R_{4m+1}} \\ \frac{r_2^2}{R_{2m+1}} & \frac{r_2^3\cos\theta_2}{R_{2m+2}} & \cdots & \frac{r_2^{m+2}\cos m\theta_2}{R_{3m+1}} & \frac{r_2^3\sin\theta_2}{R_{3m+2}} & \cdots & \frac{r_2^{m+2}\sin m\theta_2}{R_{4m+1}} \\ \vdots & \vdots & \ddots & \vdots & \vdots & \ddots & \vdots \\ \frac{r_n^2}{R_{2m+1}} & \frac{r_n^3\cos\theta_n}{R_{2m+2}} & \cdots & \frac{r_n^{m+2}\cos m\theta_n}{R_{3m+1}} & \frac{r_n^3\sin\theta_n}{R_{3m+2}} & \cdots & \frac{r_n^{m+2}\sin m\theta_n}{R_{4m+1}} \end{bmatrix},$$

$$\boldsymbol{C}=\begin{bmatrix} 0 & \frac{E_{11}}{R_1} & \vdots & \frac{E_{1m}}{R_{m-1}} & \frac{F_{11}}{R_m} & \vdots & \frac{F_{1m}}{R_{2m}} \\ 0 & \frac{E_{21}}{R_1} & \vdots & \frac{E_{2m}}{R_{m-1}} & \frac{F_{21}}{R_m} & \vdots & \frac{F_{2m}}{R_{2m}} \\ \vdots & \vdots & \ddots & \vdots & \vdots & \ddots & \vdots \\ 0 & \frac{E_{n1}}{R_1} & \vdots & \frac{E_{nm}}{R_{m-1}} & \frac{F_{n1}}{R_m} & \vdots & \frac{F_{nm}}{R_{2m}} \end{bmatrix},$$

$$\boldsymbol{D}=\begin{bmatrix} \frac{2\eta_1 r_1}{R_{2m+1}} & \frac{G_{11}}{R_{2m+2}} & \vdots & \frac{G_{1m}}{R_{3m+1}} & \frac{H_{11}}{R_{3m+2}} & \vdots & \frac{H_{1m}}{R_{4m+1}} \\ \frac{2\eta_2 r_2}{R_{2m+1}} & \frac{G_{21}}{R_{2m+2}} & \vdots & \frac{G_{2m}}{R_{3m+1}} & \frac{H_{21}}{R_{3m+2}} & \vdots & \frac{H_{2m}}{R_{4m+1}} \\ \vdots & \vdots & \ddots & \vdots & \vdots & \ddots & \vdots \\ \frac{2\eta_n r_n}{R_{2m+1}} & \frac{G_{n1}}{R_{2m+2}} & \vdots & \frac{G_{nm}}{R_{3m+1}} & \frac{H_{n1}}{R_{3m+2}} & \vdots & \frac{H_{nm}}{R_{4m+1}} \end{bmatrix}.$$

We denote Eq. (2.11) as

$$\boldsymbol{K}\boldsymbol{e}=\boldsymbol{h}. \tag{2.12}$$

The norm of the first column of $\boldsymbol{K}$ in Eq. (2.12) is $\sqrt{2m+1}$. Multiple-scale R_k can be solved

in the same way as Eq. (2.6)

$$R_k=\begin{cases}\alpha\left(\dfrac{1}{2m+1}\displaystyle\sum_{i=1}^{2m+1}\left[(r_i^k\cos k\theta_i)^2+(E_{ik})^2\right]\right)^{\frac{1}{2}}, & k=1,\cdots,m,\\ \alpha\left(\dfrac{1}{2m+1}\displaystyle\sum_{i=1}^{2m+1}\left[(r_i^k\sin k\theta_i)^2+(F_{ik})^2\right]\right)^{\frac{1}{2}}, & k=m+1,\cdots,2m,\end{cases}$$

$$R_{2m+1}=\alpha\left(\frac{1}{2m+1}\sum_{i=1}^{2m+1}\left[r_i^4+(2\eta_i r_i)^2\right]\right)^{\frac{1}{2}},$$

$$R_{2m+1+k}=\begin{cases}\alpha\left(\dfrac{1}{2m+1}\displaystyle\sum_{i=1}^{2m+1}\left[(r_i^{k+2}\cos k\theta_i)^2+(G_{ik})^2\right]\right)^{\frac{1}{2}}, & k=1,\cdots,m,\\ \alpha\left(\dfrac{1}{2m+1}\displaystyle\sum_{i=1}^{2m+1}\left[(r_i^{k+2}\sin k\theta_i)^2+(H_{ik})^2\right]\right)^{\frac{1}{2}}, & k=m+1,\cdots,2m.\end{cases}$$

For the second kind of boundary condition Eq. (2.7c), we can derive the corresponding linear algebraic system in a similar way:

$$\Delta u(r_i,\theta_i)=\frac{4c_0}{R_1^2}+\sum_{k=1}^{m}\left(\frac{c_k M_{ik}}{R_{3m+1}}+\frac{d_k N_{ik}}{R_{4m+1}}\right), \tag{2.13}$$

where

$$M_{ik}=4(k+1)r_i^k\cos k\theta_i,\quad N_{ik}=4(k+1)r_i^k\sin k\theta_i,$$

n boundary collocation points $\{(r_i,\theta_i)\}_{i=1}^n$ are used in the approximation of such boundary condition:

$$u(r_i,\theta_i)=f(r_i,\theta_i),\quad \Delta u(r_i,\theta_i)=g(r_i,\theta_i),\quad i=1,\cdots,N. \tag{2.14}$$

Put Eq. (2.10) into Eq. (2.8) and Eq. (2.14) and derive a $2n\times(4m+2)$ dimensions linear equation system similar to Eq. (2.11) as:

$$\begin{bmatrix}\boldsymbol{A} & \boldsymbol{B}\\ \boldsymbol{0} & \boldsymbol{M}\end{bmatrix}\begin{bmatrix}\boldsymbol{a}\\ \boldsymbol{b}\end{bmatrix}=\boldsymbol{K}\begin{bmatrix}\boldsymbol{a}\\ \boldsymbol{b}\end{bmatrix}=\begin{bmatrix}\boldsymbol{f}\\ \boldsymbol{g}\end{bmatrix}, \tag{2.15}$$

where

$$\boldsymbol{M}=\begin{bmatrix}\dfrac{2\eta_1 r_1}{R_{2m+1}} & \dfrac{M_{11}}{R_{2m+2}} & \vdots & \dfrac{M_{1m}}{R_{3m+1}} & \dfrac{N_{11}}{R_{3m+2}} & \vdots & \dfrac{N_{1m}}{R_{4m+1}}\\ \dfrac{2\eta_2 r_2}{R_{2m+1}} & \dfrac{M_{21}}{R_{2m+2}} & \vdots & \dfrac{M_{2m}}{R_{3m+1}} & \dfrac{N_{21}}{R_{3m+2}} & \vdots & \dfrac{N_{2m}}{R_{4m+1}}\\ \vdots & \vdots & \ddots & \vdots & \vdots & \ddots & \vdots\\ \dfrac{2\eta_n r_n}{R_{2m+1}} & \dfrac{M_{n1}}{R_{2m+2}} & \vdots & \dfrac{M_{nm}}{R_{3m+1}} & \dfrac{N_{n1}}{R_{3m+2}} & \vdots & \dfrac{N_{nm}}{R_{4m+1}}\end{bmatrix}.$$

As $\boldsymbol{K}$ should be equilibrated, R_i is derived :

$$R_k=\begin{cases}\alpha\left(\dfrac{1}{2m+1}\displaystyle\sum_{i=1}^{2m+1}\left[(r_i^k\cos k\theta_i)^2\right]\right)^{\frac{1}{2}}, & k=1,\cdots,m,\\ \alpha\left(\dfrac{1}{2m+1}\displaystyle\sum_{i=1}^{2m+1}\left[(r_i^k\sin k\theta_i)^2\right]\right)^{\frac{1}{2}}, & k=m+1,\cdots,2m,\end{cases}$$

$$R_{2m+1}=\alpha\left(\frac{1}{2m+1}\left[16(2m+1)+\sum_{i=1}^{2m+1}r_i^4\right]\right)^{\frac{1}{2}},$$

$$R_{2m+1+k}=\begin{cases}\alpha\left(\dfrac{1}{2m+1}\displaystyle\sum_{i=1}^{2m+1}\left[(r_i^{k+2}\cos k\theta_i)^2+(M_{ik})^2\right]\right)^{\frac{1}{2}}, & k=1,\cdots,m,\\ \alpha\left(\dfrac{1}{2m+1}\displaystyle\sum_{i=1}^{2m+1}\left[(r_i^{k+2}\sin k\theta_i)^2+(N_{ik})^2\right]\right)^{\frac{1}{2}}, & k=m+1,\cdots,2m.\end{cases}$$

We refer readers to [19] for further details.

3 The MFS with LOOCV algorithm

3.1 MFS solving Laplace equation

Here we consider Eq. (2.1a) with Dirichlet boundary condition Eq. (2.1b). Let $\{\boldsymbol{\xi}_k\}_{k=1}^M$ denote the source points which are located on a pseudo-boundary outside the closure of $\overline{\Omega}$. The solution to the Laplace equation (2.1a) can be approximated by a linear combination of fundamental solutions as follows:

$$u(\boldsymbol{\xi},\boldsymbol{x})=\sum_{k=1}^{M}c_kG_1(\xi_k,\boldsymbol{x}),\quad \boldsymbol{x}\in\overline{\Omega},\tag{3.1}$$

where

$$G_1(\boldsymbol{\xi},\boldsymbol{x})=-\frac{1}{2\pi}\log|\boldsymbol{\xi}-\boldsymbol{x}|\ \text{ in two dimensions.}\tag{3.2}$$

Let $\{\boldsymbol{x}_i\}_{i=1}^N$ be the collocation points on the domain boundary in the approximation, the Dirichlet boundary condition Eq. (2.1b) is rewritten as:

$$u(\xi_k,x_i)=\sum_{k=1}^{M}c_kG_1(\xi_k,x_i)=f(x_i),\quad k=1,\cdots,M,\quad i=1,\cdots,N.\tag{3.3}$$

In matrix form, we have the following $N\times M$ system of equations

$$\boldsymbol{Kc}=\boldsymbol{f},\tag{3.4}$$

where

$$\boldsymbol{K}=[G_1(\xi_k,x_i)]_{1\le i\le N,1\le k\le M},\quad \boldsymbol{f}=[f(x_1),f(x_2),\cdots,f(x_N)]^T,$$

and $\boldsymbol{c}=[c_1,c_2,\cdots,c_M]^T$ is the coefficient vector to be determined.

In the mixed Dirichlet-Neumann boundary condition:

$$u=f_1 \quad \text{on } \partial\Omega_1 \quad \text{and} \quad \frac{\partial u}{\partial n}=f_2 \quad \text{on } \partial\Omega_2, \tag{3.5}$$

M source points and N boundary collocation points are chosen, we have:

$$u(\xi_k,x_i)=f_1(x_i),\quad i=1,\cdots,N_1,\quad \frac{\partial u}{\partial n}(\xi_k,x_i)=f_2(x_i),\quad i=N_1+1,\cdots,N_1+N_2, \tag{3.6}$$

where $N=N_1+N_2$, what we obtained is still an $N\times M$ equation system equal to Eq. (3.4), where

$$K_{ik}=G_1(\xi_k,x_i),\quad f_i=f_1(x_i),\quad 1\le i\le N_1, \tag{3.7a}$$

$$K_{ik}=\frac{\partial G_1}{\partial n}(\xi_k,x_i),\quad f_i=f_2(x_i),\quad N_1+1\le i\le N_1+N_2, \tag{3.7b}$$

and $\boldsymbol{c}=[c_1,c_2,\cdots,c_M]^T$ is the coefficient vector to be determined.

3.2 MFS solving Biharmonic equation

Here we consider the biharmonic equation with two boundary conditions. The solution u can be approximated as follows:

$$u(\boldsymbol{\xi},\boldsymbol{x})=\sum_{k=1}^{M}a_kG_1(\xi_k,\boldsymbol{x})+\sum_{k=1}^{M}b_kG_2(\xi_k,\boldsymbol{x}),\quad \boldsymbol{x}\in\overline{\Omega}, \tag{3.8}$$

where G_1 is given in (3.2), and

$$G_2=-\frac{1}{8\pi}|\boldsymbol{\xi}-\boldsymbol{x}|^2\log|\boldsymbol{\xi}-\boldsymbol{x}| \text{ in two dimensions.} \tag{3.9}$$

We choose N collocation points $\{\boldsymbol{x}_i\}_{i=1}^N$ on the domain boundary $\partial\Omega$. Then the coefficient vector $\boldsymbol{a}=[a_1,\cdots,a_M]^T$ and $\boldsymbol{b}=[b_1,\cdots,b_M]^T$ can be determined by collocating the boundary conditions (2.7b) and (2.7c) as follows:

$$u(\xi_k,x_i)=f(x_i),\quad \frac{\partial u}{\partial n}(\xi_k,x_i)=g(x_i),\quad i=1,\cdots,N,\quad k=1,\cdots,M, \tag{3.10}$$

which yields a $2N\times 2M$ system

$$\boldsymbol{K}\begin{bmatrix}\boldsymbol{a}\\ \boldsymbol{b}\end{bmatrix}=\boldsymbol{K}\boldsymbol{c}=\begin{bmatrix}\boldsymbol{f}\\ \boldsymbol{g}\end{bmatrix}, \tag{3.11}$$

where in the first biharmonic problem

$$\boldsymbol{K}=\begin{bmatrix} G_1(\xi_k,x_i) & G_2(\xi_k,x_i) \\ \dfrac{\partial G_1}{\partial n}(\xi_k,x_i) & \dfrac{\partial G_2}{\partial n}(\xi_k,x_i) \end{bmatrix},$$

$\boldsymbol{f}=[f(x_1),\cdots,f(x_N)]^T$, and $\boldsymbol{g}=[g(x_1),\cdots,g(x_N)]^T$. In the second biharmonic problem, we have

$$\boldsymbol{K}=\begin{bmatrix} G_1(\xi_k,x_i) & G_2(\xi_k,x_i) \\ \Delta G_1(\xi_k,x_i) & \Delta G_2(\xi_k,x_i) \end{bmatrix}$$

and $\boldsymbol{c}=[\boldsymbol{a},\boldsymbol{b}]^T$ is the coefficient vector to be determined.

3.3 LOOCV algorithm on choosing source points

The LOOCV Algorithm was designed to choose a suitable shape parameter by Rippa [23] in the Radial Basis Function. In MFS, this algorithm is used to select suitable distance of source points to achieve relative better results. We only present the process of harmonic and non-harmonic problem in this section. Biharmonic and non-biharmonic problems are easy to be extended. Suppose the boundary curve $\partial\Omega$ is presented in polar coordinates like:

$$x=r(\theta)\cos\theta,\quad y=r(\theta)\sin\theta,\quad \theta\in[0,2\pi). \tag{3.12}$$

Discrete θ as θ_i, $i=1,\cdots,N$, then we can get corresponding $r_i=r(\theta_i)$, $i=1,\cdots,N$, which could be used to describe boundary collocation points in the approximation of boundary:

$$\boldsymbol{x}_i=r_i(\cos(\theta_i),\sin(\theta_i)),\quad i=1,\cdots,N. \tag{3.13}$$

In [1,11], we know that results would be excellent to collocate source points uniformly at fixed distance from boundary, thus we choose two approaches placing source points as follows for different boundary conditions:

1. On a circle by equal angles: When the boundary condition is harmonic, satisfied accuracy would be achieved by locating source points uniformly as a circle $\partial\tilde{\Omega}$ surrounding boundary $\partial\Omega$. Let $\theta_i=\frac{2\pi(i-1)}{N}$, $i=1,\cdots,N$, we get boundary collocation points distributed as (3.12) and source points represented as:

$$\boldsymbol{\xi}_k=R(\cos(\phi_k),\sin(\phi_k)),\quad \phi_k=\frac{2\pi(k-1)}{M},\quad k=1,\cdots,M,$$

   where $R\geq\max|\boldsymbol{r}|$ which is large enough to satisfy: $\partial\Omega\subset\partial\tilde{\Omega}$.

2. At fixed distance from boundary by equal segments: In order to collocate source points by equal segments, we should determine uniform boundary collocation points at first. The length S of boundary curve is calculated by :

$$S=\int_0^{2\pi}\sqrt{r(\theta)^2+r'(\theta)^2}d\theta,$$

then, each segment between neighboring boundary collocation points are equal to S/N. Let $\theta_1=0$, then the component $t=\theta_{i+1}$ of next element is achieved in order by solving:

$$\sqrt{(r(t)\cos t+r(\theta_i)\cos\theta_i)^2+(r(t)\sin t+r(\theta_i)\sin\theta_i)^2}-\frac{S}{N}=0,\quad i=1,\cdots,N-1.$$

Put θ_i, $i=1,\cdots,N-1$, into (3.13), boundary collocation points are evaluated. Outward normal vector of each boundary collocation points are defined as:

$$\boldsymbol{n}_i=\frac{1}{\sqrt{r^2(\theta_i)+r'^2(\theta_i)}}(r'(\theta_i)\sin\theta_i+r(\theta_i)\cos\theta_i,r(\theta_i)\sin\theta_i-r'(\theta_i)\cos\theta_i),$$

where $i=1,\cdots,N$. The number of source points and boundary collocation points are M and N respectively. Let $M=N/\mu$ and μ is an integer, source points could be placed along outward normal vectors at distance h as follows:

$$\boldsymbol{\xi}_k=\boldsymbol{x}_{\mu(k-1)+1}+h\boldsymbol{n}_{\mu(k-1)+1},\quad j=1,\cdots,M.$$

The right hand side of (3.4) f is calculated through these points and the coefficient vector $\boldsymbol{c}$ is achieved through (3.4).

Let

$$E_1(t)=\|\widetilde{\boldsymbol{K}}\boldsymbol{c}-\tilde{f}\|,$$

where t equals to R or h depending on harmonic problem or non-harmonic problem, $\widetilde{\boldsymbol{K}}$ and $\tilde{f}$ are reconstructed by source points and test points which are different from collocation points on the boundary.

$$E_2(t)=\|e(t)\|$$

is the error function in the process of Leave-one-out Cross Validation, where

$$e(t)=[e_1(t),e_2(t),\cdots,e_M(t)]\quad\text{and}\quad e_j(t)=\frac{c_j(t)}{\widetilde{k}_{jj}(t)},\quad j=1,\cdots,M,$$

$\widetilde{k}_{jj}(t)$ are the diagonal elements of matrix $\widetilde{\boldsymbol{K}}^{-1}$. LOOCV algorithm will search the best value of t in given search interval by re-calculating $\widetilde{\boldsymbol{K}}$ and $\tilde{f}$ for each t, until satisfying that $E_1(t)$ is as small as possible. Then coefficient vector c is determined and could be used to evaluate test points.

4 Numerical examples

To compare the performance of the MFS and the Trefftz Method, we consider four two-dimensional problems. In this section, n_b, n_s, n_t denotes the number of boundary points, source points, and test points, respectively. According to the Maximum Principle [22], the

maximum error would occur on the boundary. Hence, test points and collocation points are selected on the boundary where the boundary values are known. The accuracy is calculated by the root-mean-square error (RMSE) which is defined as follows:

$$RMSE=\sqrt{\frac{1}{n_t}\sum_{i=1}^{n_t}(\bar{u}_i(x_i,y_i)-u_i(x_i,y_i))^2}, \tag{4.1}$$

where u_i and $\bar{u}_i$ are the exact solution and approximation solution, respectively.

As shown in Fig. 1, five irregular domains are considered in this section. The parametric equation of the boundary $\partial\Omega$ is defined as follows:

$$\partial\Omega=\{(x,y)|x=r(\theta)\cos(\sigma(\theta)),\quad y=r(\theta)\sin(\sigma(\theta)),\quad 0\leq\theta<2\pi\}, \tag{4.2}$$

where $r(\theta)$ depends of the given domain. They are

1. Cassini domain:

$$r(\theta)=\left(\cos(4\theta)+\sqrt{\frac{18}{5}-\sin^2(4\theta)}\right)^{1/3},\quad \sigma(\theta)=\theta.$$

2. Amoeba-like domain:

$$r(\theta)=e^{\sin\theta}\sin^2(2\theta)+e^{\cos\theta}\cos^2(2\theta),\quad \sigma(\theta)=\theta.$$

3. Cardioid domain:

$$r(\theta)=\frac{\sqrt{c^2+\left|\sin\left(\frac{\theta}{2}\right)\right|}}{\sqrt{c^2+1}},\quad c=0.3218,\quad \sigma(\theta)=\theta.$$

4. L-shaped domain: No parametric equation is available in this case.

5. Gear-shaped domain:

$$r(\theta)=2+\frac{1}{2}\sin(7\theta),\quad \sigma(\theta)=\theta+\frac{1}{2}\sin(7\theta).$$

For the MFS, collocation points are uniformly distributed on the boundary.When the boundary condition is harmonic, source points are placed on a circle covering the domain. See Fig. 2a. When the imposed boundary condition is non-harmonic, source points are selected on a fictitious boundary with similar shape that is close to the boundary as shown in Fig. 2b. To find a suitable distance from source points to the boundary points, we apply the Leave-One-Out cross validation (LOOCV) algorithm. We refer readers to [1] for further details.

For the Trefftz Method, just boundary collocation points on the boundary are sufficient. To reduce the condition number, the multiple scale technique is required in the implementation of the Trefftz method.

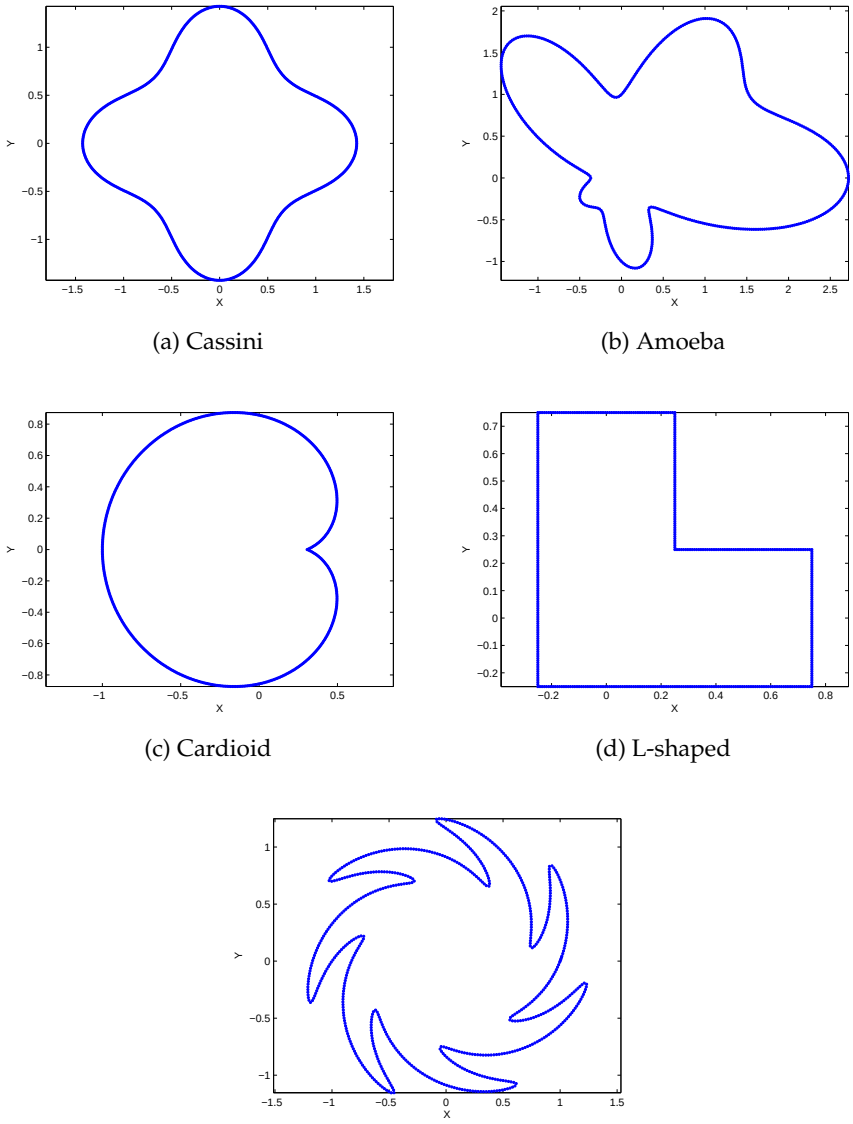

(a) Cassini (b) Amoeba

(c) Cardioid (d) L-shaped

(e) Gear-shaped

Figure 1: The profiles of five different irregular domains.

Example 4.1. We consider the Laplace equation (2.1a) with the Dirichlet boundary condition (2.1b)

$$f(x,y)=e^x\sin(y),\quad (x,y)\in\partial\Omega. \tag{4.3}$$

Since the boundary condition is harmonic, the exact solution is given as

$$u(x,y)=e^x\sin(y),\quad (x,y)\in\hat{\Omega}. \tag{4.4}$$

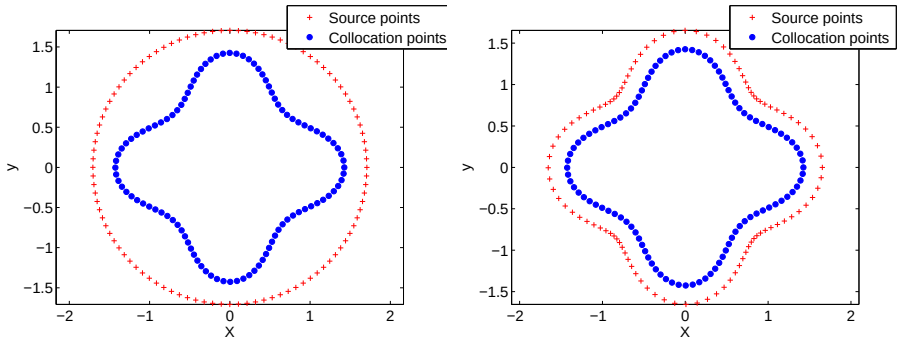

(a) Harmonic boundary condition (b) Nonharmonic boundary condition

Figure 2: The distribution of source points of the MFS for harmonic boundary condition and nonharmonic condition.

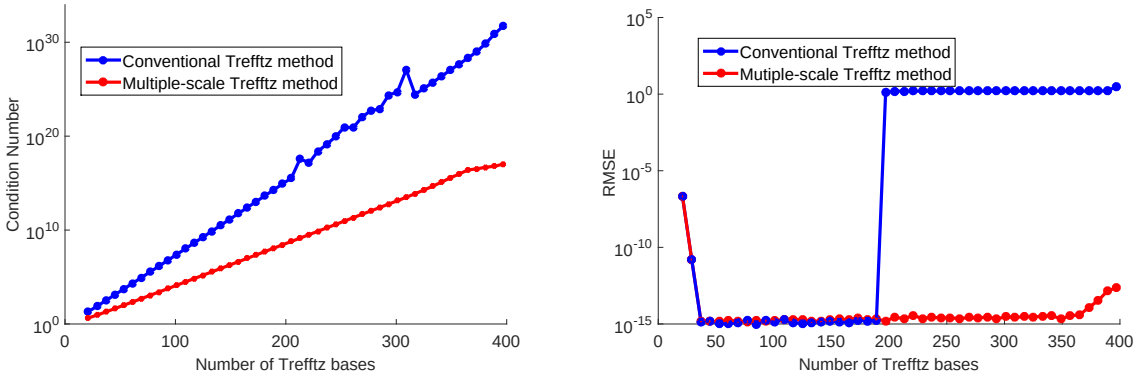

(a) Condition number (b) Error

Figure 3: Example 4.1: The profiles of condition numbers and errors with and without the multiple scale method using the Trefftz method.

First, we consider the Cassini domain (see Fig. 1a). Table 1 shows the results of the MFS with LOOCV using various numbers of collocation and source points, and r is the maximal distance from the geometry center to the boundary. In [1], the number of collocation points and source points are equal. In our approach, we find that similar accuracy can be achieved using less source points which implies less computational time.

For the Trefftz method, b denotes the number of a group of Trefftz bases of the Laplace operator. Fig. 3 shows the profiles of condition numbers and errors with and without using the multiple scale method. Without using the multiple scale method, the condition number grows proportional to the number of basis functions of the Trefftz method and will quickly go out of control. With the multiple scale method, the solutions are stable and reliable. From Table 2, we observe that the accuracy obtained by using the Trefftz method is as good as the MFS.

Table 1: Example 4.1: The RMSE for various numbers of collocation and source points using the MFS with LOOCV.

n_b	n_s	Search interval	R	RMSE	CPU time
200	100	$(r,2r)$	2.0912	1.5347e-15	0.5775
200	200	$(r,2r)$	2.0912	3.2416e-14	0.5482
500	250	$(r,2r)$	2.2306	1.0774e-15	1.1850
500	500	$(r,2r)$	2.2306	2.3187e-14	1.2500

Table 2: Example 4.1: The corresponding RMSE for various orders of Trefftz bases.

n_b	b	RMSE	CPU time	b	RMSE	CPU time
200	21	2.1041e-07	0.4490	41	1.1180e-15	0.4206
200	61	1.0925e-15	0.4100	81	2.2615e-15	0.3998
200	101	1.3175e-15	0.4004			
500	21	2.1041e-07	0.8974	41	1.4824e-15	0.7884
500	61	1.7412e-15	0.7879	81	1.4551e-15	0.7908
500	101	1.7551e-15	0.7985			

Table 3: Example 4.1: Comparison between Trefftz Method and MFS.

	Trefftz Method		MFS		
Domain Shape	b	RMSE	Search interval	R	RMSE
Amoeba	61	3.2709e-15	$(r,6r)$	3.6272	5.5387e-15
Cassini	77	1.4079e-10	$(r,6r)$	2.6736	1.1521e-15
Cardioid	45	3.7126e-15	$(r,2r)$	1.5774	5.8688e-16
L-shaped	29	1.7276e-15	$(r,5r)$	0.9783	6.3606e-16
Gear-shaped	37	8.9747e-16	$(r,4r)$	2.6822	4.8016e-15

In Table 3, we compare these two methods for various domains as shown in Fig. 1. For the MFS, we choose $n_b = n_s = 500$, and $n_t = 400$. From the results in these three tables, we conclude both methods are equally effective in terms of accuracy. However, we prefer the MFS due to its simplicity in numerical implementation.

Example 4.2. We consider the Laplace equation Eq. (2.1a) with Dirichlet boundary condition Eq. (2.1b), where $f(x,y) = x^2y^3$.

We consider Ω to be the amoeba domain as shown in Fig. 1b. The number of test points is $n_t = 400$. d is the maximum distance between the two neighboring collocation points. To improve the accuracy, an equal number of source points are located at a fixed distance h from the boundary.

For the Trefftz method, we select the same number of collocation points. As shown in Fig. 4, we present the profiles of condition number and error with and without using the multiple scale method. In the case of a non-harmonic boundary condition, the condition number without using the multiple scale method is even worse than Fig. 3 in Example 4.1. The multiple scale method works nicely to alleviate the difficulty of the extremely

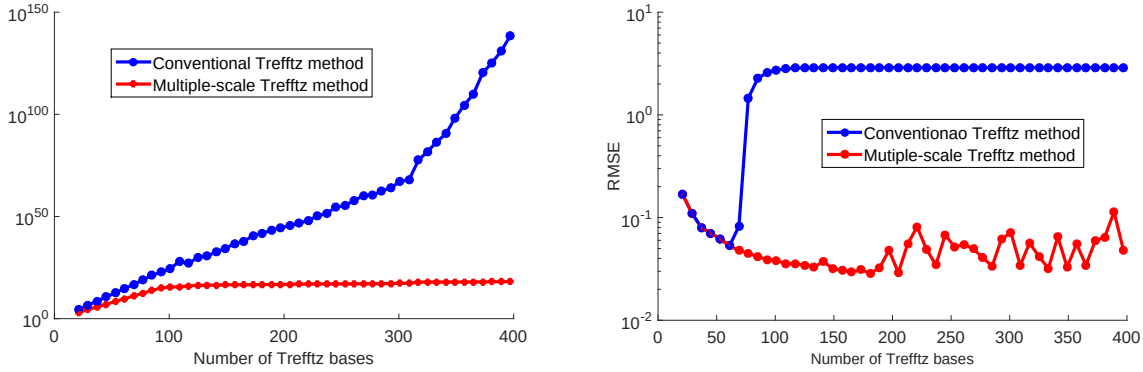

(a) Condition number (b) Error

Figure 4: Example 4.2: The profiles of condition numbers and errors with and without the multiple scale method using the Trefftz method.

high condition number for the Trefftz method.

Table 4 and Table 5 show the results of both the Trefftz method and the MFS in the amoeba domain. In Table 6, we compare the accuracy of these two methods for various irregular domains shown in Fig. 1.

Overall, the MFS is superior to the Trefftz method in terms of accuracy. The better accuracy of the MFS is at the expense of a searching algorithm for the optimal source location using LOOCV. But even with such additional cost, the computational cost of both methods is not much different. Despite the advantage of simplicity, the need of searching for the optimal location of the source points presents a disadvantage for the MFS. With the LOOCV, we are able to overcome such shortcoming at a reasonable cost.

Table 4: Example 4.2: The RMSE for the MFS.

n_b	n_s	Search interval	h	RMSE	CPU (sec)
200	100	$(0,2d)$	0.0986	6.3193e-03	0.4530
200	200	$(0,2d)$	0.0573	2.0230e-03	0.5558
500	250	$(0,2d)$	0.0461	9.5285e-04	0.8945
500	500	$(0,2d)$	0.0319	1.8133e-04	1.0421

Table 5: Example 4.2: The RMSE for various Trefftz basis.

n_b	b	RMSE	CPU (sec)	b	RMSE	CPU (sec)
200	21	1.6697e-01	0.4093	41	7.7712e-02	0.4393
200	61	5.2798e-02	0.4244	81	4.1350e-02	0.4171
200	101	4.2359e-02	0.4261			
500	21	1.6706e-01	0.8180	41	7.7725e-02	0.8345
500	61	5.2803e-02	0.8125	81	4.1337e-02	0.7967
500	101	3.7120e-02	0.7879			

Table 6: Example 4.2: Comparison between the Trefftz Method and the MFS.

	Trefftz Method		MFS		
Domain Shape	b	RMSE	Search interval	h	RMSE
Amoeba	181	2.8754e-02	$(0,4d)$	0.0319	1.9053e-04
Cassini	309	1.7137e-09	$(0,8d)$	0.1208	3.0628e-16
Cardioid	189	7.1715e-05	$(0,2d)$	0.0149	9.2327e-06
L-shaped	301	8.3291e-05	$(0,2d)$	0.0110	1.6524e-05
Gear-shaped	173	1.8170e-02	$(0,4d)$	0.0385	3.7522e-03

Example 4.3. In this example, we consider the following biharmonic problem:

$$\Delta^2 u = 0, \qquad (x,y) \in \Omega, \tag{4.5a}$$

$$u(x,y) = x^2 y^3, \qquad (x,y) \in \partial\Omega, \tag{4.5b}$$

$$\Delta u(x,y) = 2y^3 + 6x^2 y, \qquad (x,y) \in \partial\Omega, \tag{4.5c}$$

where Ω is a Cardioid domain.

In this example, $n_b = 500$ and $n_t = 201$ are chosen for all the tests. For the MFS, the source points are placed very close to the boundary with distance h. d is the maximum distance between two neighboring collocation points. For the Trefftz method, we use various numbers of biharmonic T-complete functions to approximate the solution u.

From Table 7 and Table 9, we notice that the optimal source points are very close to the physical boundary. This is consistent with the results obtained in [1]. Comparing the results in Tables 7 and 8, it is clear that the MFS is again superior to the Trefftz method in terms of accuracy, but the Trefftz method consumes less CPU time. For the MFS in Table 9, we choose the same number of boundary points and source points. For four domains as shown in Table 9, it is clear that the MFS is far superior to the Trefftz method in terms of accuracy.

Table 7: Example 4.3: The RMSE for the MFS.

n_b	n_s	Search interval	h	RMSE	CPU (sec)
500	250	$(0,8d)$	0.0532	1.9268e-05	2.2007
500	500	$(0,8d)$	0.0126	5.9034e-06	7.6547

Table 8: Example 4.3: The RMSE for the Trefftz method.

n_b	b	RMSE	CPU (sec)	b	RMSE	CPU (sec)
500	22	2.2171e-02	1.1304	62	7.6066e-03	1.1510
500	102	5.0891e-03	1.3474	142	3.9934e-03	1.2173
500	182	3.3632e-03	1.2053			

Example 4.4. We consider the equation

$$\Delta^2 u(x,y) = 0,$$

Table 9: Example 4.3: Comparison between Trefftz Method and MFS.

	Trefftz Method		MFS		
Domain Shape	b	RMSE	Search interval	h	RMSE
Amoeba	102	4.4621e-01	$(0,6d)$	0.0468	5.8614e-04
Cassini	302	3.5904e-05	$(0,7d)$	0.1136	1.1701e-14
Cardioid	402	2.3626e-03	$(0,6d)$	0.0119	4.3087e-06
Gear-shaped	322	3.1621e-01	$(0,4d)$	0.0312	6.8960e-03

with the first biharmonic boundary conditions

$$u(x,y)=x^2y^3, \qquad (x,y)\in\partial\Omega, \tag{4.6a}$$

$$\frac{\partial u}{\partial \mathbf{n}}=(\nabla x^2y^3)\cdot\mathbf{n}, \qquad (x,y)\in\partial\Omega. \tag{4.6b}$$

To study the stability of these two methods, the boundary conditions are disturbed by random noise for the Gear-shaped domain. We utilize the MATLAB function *Rand* to generate random noise $Ran\in[-1,1]$. Let $\{(x_i,y_i)\}_{i=1}^{n_b}$ be the boundary collocation points, and $\tilde{u}$ and $\partial\tilde{u}/\partial\mathbf{n}$ be the perturbed boundary conditions which can be explicitly expressed as follows:

$$\tilde{u}(x_i,y_i)=u(x_i,y_i)+\left|\max_{1\le i\le n_b}(u(x_i,y_i))-\min_{1\le i\le n_b}(u(x_i,y_i))\right|*s*Ran,$$

$$\frac{\partial\tilde{u}}{\partial\mathbf{n}}(x_i,y_i)=\frac{\partial u}{\partial\mathbf{n}}(x_i,y_i)+\left|\max_{1\le i\le n_b}\left(\frac{\partial u}{\partial\mathbf{n}}(x_i,y_i)\right)-\min_{1\le i\le n_b}\left(\frac{\partial u}{\partial\mathbf{n}}(x_i,y_i)\right)\right|*s*Ran,$$

where $i=1,2,\cdots,n_b$ and s is the level of noise.

For the numerical implementation, we choose $n_b=n_s=500$, $n_t=201$. The noise level is chosen $s=3\%$. As shown in Table 10, the numerical results obtained by the MFS are very stable for various search intervals using LOOCV. From Tables 10 and 11, we observe that the Trefftz method can not achieve the same level of accuracy as the MFS. From Table 12, we show that the MFS is far superior to the Trefftz method in accuracy for four irregular domains. This is consistent with the results obtained in Examples 4.2 and 4.3. We also notice that for the Cassini domain, we consistently obtain a highly accurate solution regardless of the types of differential equations and boundary conditions we have tested. We believe the main reason is due to the symmetry and the high smoothness of the boundary of the Cassini domain.

5 Conclusions

In this paper, we make comparisons of two powerful boundary meshless methods: the Trefftz method and the MFS. We consider the Laplace and biharmonic equations for five irregular domains. To enhance the performance of these two methods, we apply the LOOCV algorithm to choose optimal source location. For the Trefftz, the multiple scale

Table 10: Example 4.4: The RMSE for the MFS with and without random noise on the boundary.

	No noise			noise		
n_b	Search interval	d	RMSE	Search interval	d	RMSE
500	$(0,2d)$	0.0122	7.0168e-04	$(0,2d)$	0.0156	1.7787e-02
500	$(0,4d)$	0.0126	7.1769e-04	$(0,4d)$	0.0408	4.4635e-02
500	$(0,6d)$	0.0138	7.2228e-04	$(0,6d)$	0.0094	2.1809e-02
500	$(0,8d)$	0.0139	7.4044e-04	$(0,8d)$	0.0071	1.8371e-02

Table 11: Example 4.4: The RMSE for the Trefftz method with random noise on the boundary.

	No noise		noise	
n_b	b	RMSE	b	RMSE
500	22	6.7088e-02	22	7.5930e-02
500	102	2.6309e-02	102	4.6118e-02
500	182	1.7339e-02	182	4.4077e-02
500	262	1.7179e-02	262	4.5035e-02
500	342	4.3316e-02	342	1.0278e-01

Table 12: Example 4.4: Comparison of the Trefftz method and the MFS.

	Trefftz Method		MFS		
Domain Shape	b	RMSE	Search interval	h	RMSE
Amoeba	342	3.4405e-02	$(0,4d)$	0.0428	1.1606e-05
Cassini	402	6.3332e-07	$(0,4d)$	0.0621	8.3928e-12
Cardioid	342	2.1181e-04	$(0,4d)$	0.0102	3.8632e-06
Gear-shaped	242	4.2832e-02	$(0,4d)$	0.0108	7.1520e-04

technique is implemented to reduce its severe ill condition numbers. For the harmonic boundary condition, these two methods are equally powerful. For the nonharmonic boundary condition, the MFS is clearly superior to the Trefftz method in terms of accuracy. For the biharmonic equation, we have the similar conclusion. For the boundary condition with noise, the Trefftz method is more stable that the MFS. Another important advantage of the MFS is its simplicity in numerical implementation. The fundamental solution of the MFS is simpler than the Trefftz method. The recent advances in the selection of the source location using the LOOCV has put the MFS in an even better position to compete with other established boundary meshless methods. Hence, as far as the numerical computation is concerned, we conclude the MFS is superior to the Trefftz method in the two dimensional case.

Acknowledgements

Authors acknowledge the support of the Soft Science Project of Shanxi Province of China (Project No. 2016041029-5), the National Natural Science Foundation of China (Grant No. 11472184) and the National Youth Science Foundation of China (Grant No. 11401423).

References

[1] C. S. CHEN, A. KARAGEORGHIS, AND Y. LI, *On choosing the location of the sources in the MFS*, Numer. Algorithms, (2015), pp. 1–24.

[2] J. T. CHEN, C. S. WU, Y. T. LEE, AND K. H. CHEN, *On the equivalence of the Trefftz method and method of fundamental solutions for Laplace and biharmonic equations*, Comput. Math. Appl., 53 (2007), pp. 851–879.

[3] G. FAIRWEATHER AND A. KARAGEORGHIS, *The method of fundamental solutions for elliptic boundary value problems*, Adv. Comput. Math., 9(1-2) (1998), pp. 69–95.

[4] Z. J. FU, W. CHEN, AND H. T. YANG, *Boundary particle method for Laplace transformed time fractional diffusion equations*, J. Comput. Phys., (235) (2013), pp. 52–66.

[5] Z. J. FU AND Q. H. QIN, *Three boundary meshless methods for heat conduction analysis in nonlinear FGMs with Kirchhoff and Laplace transformation*, Adv. Appl. Math. Mech., 4(5) (2012), pp. 519–542.

[6] M. A. GOLBERG AND C. S. CHEN, *The method of fundamental solutions for potential, Helmholtz and diffusion problems*, in M. A. Golberg, editor, Boundary Integral Methods: Numerical and Mathematical Aspects, WIT Press, 1998, pp. 103–176.

[7] P. GORZELAŃCZYK AND J. A. KOŁODZIEJ, *Some remarks concerning the shape of the source contour with application of the method of fundamental solutions to elastic torsion of prismatic rods*, Eng. Anal. Boundary Elem., 32(1) (2008), pp. 64–75.

[8] J. A. KOLODZIEJ AND A. P. ZIELINSKI, *Boundary collocation method applied to non-linear conditions*, in Boundary Collocation Techniques and Their Application in Engineering, WIT Press, 2009.

[9] V. D. KUPRADZE AND M. A. ALEKSIDZE, *The method of functional equations for the approximate solution of certain boundary value problems*, Comput. Math. Math. Phys., 4 (1964), pp. 82–126.

[10] Z. C. LI, T. T. LU, H. Y. HU, AND H. D. CHENG, *The collocation Trefftz method*, in Trefftz and Collocation Methods, WIT Press, 2008.

[11] M. LI, C. S. CHEN, AND A. KARAGEORGHIS, *The MFS for the solution of harmonic boundary value problems with non-harmonic boundary conditions*, Comput. Math. Appl., 66 (2013), pp. 2400–2424.

[12] Z. C. LI, T. T. LU, H. T. HUANG, AND A. H. D. CHENG, *Trefftz, collocation, and other boundary methods–a comparison,* Numer. Math. Partial Diff. Equations, 23(1) (2007), pp. 93–144.

[13] C. S. LIU, *An effectively modified direct Trefftz method for 2D potential problems considering the domain's characteristic length*, Eng. Anal. Boundary Elem., 31(12) (2007), pp. 983–993.

[14] C. S. LIU, *A modified Trefftz method for two-dimensional Laplace equation considering the domain's characteristic length*, CMES Comput. Model. Eng. Sci., 21(1) (2007), pp. 53–65.

[15] C. S. LIU, *A highly accurate MCTM for direct and inverse problems of biharmonic equation in arbitrary plane domains*, CMES Comput. Model. Eng. Sci., 30(2) (2008), pp. 65–75.

[16] C. S. LIU, *Improving the ill-conditioning of the method of fundamental solution for 2d Laplace equation*, CMES Comput. Model. Eng. Sci., 28 (2008), pp. 77–93.

[17] C. S. LIU, *A modified collocation Trefftz method for the inverse Cauchy problem of Laplace equation*, Eng. Anal. Boundary Elem., 32(9) (2008), pp. 778–785.

[18] C. S. LIU, *An equilibrated method of fundamental solutions to choose the best source points for the Laplace equation*, Eng. Anal. Boundary Elem., 36(8) (2012), pp. 1235–1245.

[19] C. S. LIU, *A multiple-scale Trefftz method for an incomplete Cauchy problem of biharmonic equation*, Eng. Anal. Boundary Elem., 37(11) (2013), pp. 1445–1456.

[20] C. S. LIU AND S. N. ATLURI, *Numerical solution of the Laplacian Cauchy problem by using a*

better postconditioning collocation Trefftz method, Eng. Anal. Boundary Elem., 37(1) (2013), pp. 74–83.

[21] R. MATHON AND R. L. JOHNSTON, *The approximate solution of elliptic boundary-value problems by fundamental solutions*, SIAM J. Numer. Anal., 14(14) (1977), pp. 638–650.

[22] M. H. PROTTER AND H. F. WEINBERGER, Maximum principles in differential equations, Englewood Cliffs, 2 (1967), pp. 177–179.

[23] S. RIPPA, *An algorithm for selecting a good value for the parameter c in radial basis function interpolation*, Adv. Comput. Math., 11(2) (1999), pp. 193–210.

[24] R. SCHABACK, *Adaptive numerical solution of MFS systems*, in The Method of Fundamental Solutions–A Meshless Method, volume 17, pages 1–27, Dynamic Publishers, 2007.

[25] T. SHIGETA, D. L. YOUNG, AND C. S. LIU, *Adaptive multilayer method of fundamental solutions using a weighted greedy QR decomposition for the Laplace equation*, J. Comput. Phys., 231(21) (2012), pp. 7118–7132.

[26] E. KITA AND N. KAMIYA, *Trefftz method: an overview*, Adv. Eng. Software, 24 (1995), pp. 3–12.

[27] E. TREFFTZ, *Ein gegenstück zum ritzschen verfahren*, Proc. 2nd Int. Cong. Appl. Mech., Zurich, (1926), pp. 131–137.